Recent Progresses on Designable Hybrids with Stimuli-Responsive Optical Properties Originating from Molecular Assembly Concerning Polyhedral Oligomeric Silsesquioxane

Masayuki Gon, Kazuo Tanaka* and Yoshiki Chujo

Department of Polymer Chemistry, Graduate School of Engineering, Kyoto University Katsura, Nishikyo-ku, Kyoto 615-8510, Japan

E-mail: tanaka@poly.synchem.kyoto-u.ac.jp

Key words: silsesquioxane; sensor; luminochromism; molecular assembly

Masayuki Gon

Masayuki Gon earned his Ph.D. in Polymer Chemistry from Kyoto University in 2016. He developed three-dimensionally-arranged π-conjugated materials and studied their specific optical and physical properties based on structure and chirality. He worked as a visiting research fellow in the group of Prof. Kenneth J. Wynne at Virginia Commonwealth University in America, in 2014. Now, he is an assistant professor of Department of Polymer Chemistry, Graduate School of Engineering, Kyoto University since 2016. His present research theme is development of functional π-conjugated materials focused on unique nature of heteroatoms.

Kazuo Tanaka

Kazuo Tanaka received his Ph.D. degree in 2004 from Kyoto University, and worked in Stanford University, USA, Kyoto University, and RIKEN as a postdoctoral fellow. In 2007, he has moved to the Department of Polymer Chemistry, Graduate School of Engineering, Kyoto University, and in 2018, he was promoted to Professor. His research projects especially focus on design of new functional materials relating optics and nanotechnology based on the heteroatom-containing conjugated polymers and organic-inorganic polymer hybrids.

Yoshiki Chujo

Yoshiki Chujo completed his Ph.D. at Kyoto University in 1980 and then joined Nagoya University as an assistant professor in 1981. In 1983, he joined the group of J. McGrath at Virginia Polytechnic Institute as a postdoctoral research fellow. He returned to Kyoto University as a lecturer in 1986 and

has been Professor of Polymer Chemistry there since 1994. In 2018, he retired from Kyoto University and was granted the title of professor emeritus. His research interests focus on polymer synthesis, inorganic polymers, and polymeric hybrid materials.

Abstract

In this review, we describe recent progresses on the stimuli-responsive hybrid materials based on polyhedral oligomeric silsesquioxane (POSS) and their applications as a chemical sensor. In particular, we explain the unique functions originating from molecular assembly concerning POSS-containing soft materials mainly from our studies. POSS has an inorganic cubic core composed of silicon–oxygen (Si–O) bonds and organic substituents at each vertex. Owing to intrinsic properties of POSS, such as high thermal stability, rigidity, and low chemical reactivity, various robust hybrid materials have been developed. From the numerous numbers of POSS hybrids, we herein focus on the environment-sensitive optical materials in which molecular assembly of POSS itself and functional units connected to POSS should be a key factor for expressing material properties. We also explain the mechanisms of chemical sensors originating from these stimuli-responsive optical properties. Stimuli-responsive excimer emission and pollutant detectors, nanoplastic sensors with the water-dispersive POSS networks, *trans* fatty acid sensors, turn-on luminescent sensors for aerobic condition and fluoride anion sensors are described. We also mention the mechanochromic polyurethane hybrids and the thermally-durable mechanochromic luminescent materials. The roles of the unique optical properties from soft materials composed of rigid POSS, which doesn't have significant light-absorption and emission properties in the visible region, are surveyed.

1. Introduction

Quality of our lives can be improved by getting information from environment. We conventionally check environmental factors, such as temperature, moisture, weather, and so on via various media. Moreover, we can also assess our health status from several vital signs, such as body temperature and blood pressure by medical examination. By utilizing imaging probes, further information can be extracted at the molecular scale. In principle, existence of the target molecules, change in microenvironmental factors and degree of reaction progresses are detected and translated to meaningful information by chemical sensors. For this purpose, stimuli-responsive materials can be directly used for collecting desired data by converting chemical and physical stimulus to detectable information such as electronic and spectral signals including color changes.[1] Various types of stimuli-responsive materials are developed so far, and among them, organic compounds are advantageous for tailor-made design to detect the targets because of flexibility in material design.[2]

Recently, we have proposed the new concept for material designs as an "element-block material".[3] The minimum functional unit including heteroatoms is defined as an "element-block", and creation of organic–inorganic hybrids was attempted by connecting and combining the element-blocks. As one of the element-blocks, polyhedral oligomeric silsesquioxane (POSS) is known (Figure 1).[4] The cubic inorganic core and organic substituents at each vertex can construct 3D architecture having various functionalities. Owing to the wide molecular designability and the resulting functional materials, POSS is regarded as a platform for constructing “designable hybrid materials”.[5] In particular, owing to intrinsic properties, such as high thermal stability, rigidity, and low chemical reactivity, various robust hybrid materials

have been developed. By loading POSS onto polymers with or without covalent bonds, thermal and mechanical reinforcement in the polymer matrices was observed.[6] This means that robust hybrid materials can be readily obtained simply by mixing POSS into polymer matrices. Thus, POSS is regarded as an element-block for hybrid formation.

Figure 1

By introducing POSS into soft materials, stimuli-responsive hybrids can be obtained. In the previous studies on such “soft hybrids”, it has been revealed that POSS can play a critical role in material properties. We showed that the POSS-core dendrimers can capture various types of aromatic compounds and dyes and maintain apparent dispersibility under biological conditions.[7] It should be mentioned that larger amounts of gest molecules can be encapsulated into the second generation, which is relatively small toward conventional vesicles, of the POSS-core dendrimer compared to polyamideamine (PAMAM) dendrimers.[8] These results suggest that the cubic and sphere-like 3D structure of POSS ensured the space to encapsulate the guest molecules even in the low generation, and tight adsorption of aromatic compounds onto the hydrophobic POSS core occurs. Based on the superior encapsulation ability of the POSS-core dendrimer, the series of biotechnology applications have been achieved. It was found that encapsulated dyes showed high resistance toward photodegradation.[8a] By suppressing molecular motions of gadolinium ions by the complexation, magnetic interaction toward water molecules can be enhanced in the NMR measurement.[9] By utilizing this effect, highly-sensitive MRI contrast agents can be obtained with the POSS-based hybrid chelators. From these studies, it has been gradually revealed that

molecular assembly of POSS itself and functional units connected to POSS often shows characteristic behaviors. In particular, by the combination with dyes, unique stimuli-responsive optical materials can be obtained.

Guanosine triphosphate (GTP) has been encapsulated by the ligand-tethered POSS-core dendrimer.[10] Since hydrogen bonding is enhanced under hydrophobic conditions in the dendrimer, complexation between the guanine base and the ligand through hydrogen bonding should be stabilized. By tuning the hydrogen bonding pattern in the ligand, other types of nucleoside triphosphates can be captured with the POSS networks.[11] By extending this research, light-driven GTP oxidase can be constructed by coexisting photocatalyst for oxidation of GTP as well as the ligand for recruiting GTP in the POSS networks.[12] These results mean that multiple functions, such as encapsulation, molecular recognition and reaction, can be tandemly realized according to the preprogrammed design in the POSS-containing molecular assembly.

As another example, paramagnetic metal complexes onto the fluorinated POSS-core dendrimer were prepared.[13] In the presence of the ligand molecule which can make coordination with the metal ion, molecular assembly was detected. Correspondingly, significant enhancement of the paramagnetic relaxation effect in ^{19}F NMR measurements was observed. Based on this system, the trace amount of bio-significant molecules, which can also work as a ligand for metal ions, can be detected with ^{19}F NMR spectrometry. By utilizing molecular assembly, detection sensitivity of MR probes can be dramatically improved. It is noted that precipitation was hardly observed in these experiments although aggregation should be formed and POSS itself has high hydrophobicity. It is proposed that POSS should play a significant role in maintaining solvent dispersibility because of the steric hindrance of

radially-distributed substituents at the vertices of POSS.

As mentioned above, it can be said that POSS soft materials are a potential platform for designing sensitive chemical sensors in which molecular assembly is a key factor for expressing stimuli-responsivity. From this viewpoint, we herein review recent progresses on the stimuli-responsive hybrid materials based on POSS and their applications as a chemical sensor. So far, a large number of review papers have been published on POSS hybrid, and various stimuli-responsive materials are introduced. We explain stimuli-responsivity originating from molecular assembly concerning POSS-containing soft materials mainly from our studies (Table 1). The series of sensors for sodium dodecyl sulfate (SDS), nanoplastics, *trans* fatty acid and fluoride anion are described. We also illustrate the optical properties of the mechanochromic polyurethane hybrids and the thermally-durable mechanochromic luminescent materials. The roles of POSS in these materials are explained.

Table 1

2. Synthesis and Design Concept of POSS

The representative synthetic schemes of POSS derivatives are summarized in Figure 2. The POSS cages can be prepared by a condensation reaction of siloxanes (R^1-Si$(OR)_3$).[4a,14] The general formula of POSS is $(RSiO_{1.5})_n$, abbreviated as R_nT_n in which organic substituents (R) are modified at silicon of the POSS cage. Various types of POSS cages are obtained depending on the reaction condition, and the most major shape is cubic structure (R_8T_8). T_8 cage is synthesized by the condensation reaction of siloxanes for several days as the precipitates because of high crystallinity of the cubic cage. (Figure 2a).[15] Incomplete POSS is also prepared in the presence of lithium hydroxide (LiOH) as lithium-templated method from siloxanes,[16] and the sequent corner capping reaction provides mono-functional POSS derivatives (Figure 2b).[17] The same incomplete POSS structures can be synthesized from the complete POSS by using corner opening reaction with tetraethylammonium hydroxide (Et_4NOH) (Figure 2c).[18] Recently, the selective corner opening reaction has been developed to obtain di-functional POSS derivatives.[19] Chemical modification is required for construction of functional POSS derivatives, however it is difficult because T_8 structure has 8 reaction points. Therefore, high reactive chemical reactions should be suitable for the synthesis. The representative chemical reactions are listed in Figure 2d. Amino-POSS, which is usually isolated as ammonium salts, is used for condensation reactions to construct amide[20] or imine linkages.[21] The Menshutkin reaction[22] is available for the POSS formation with dimethylamine group (DMA-POSS) to create ammonium salts connected functional groups.[23] Vinyl-POSS is applied for both the thiol-ene reaction as click chemistry[24] and the Mizoroki–Heck reaction[25] with metal catalytic condition to extend π-conjugated system for luminescent derivatives.[26] Iodo-POSS (I-POSS) is

obtained by iodization of phenyl groups[27] and that is readily used for cross-coupling reactions.[28,29] We also succeeded in preparing boronic esters via lithiation of I-POSS.[30] Thiol-POSS is useful for extension of the chain length by the thiol-ene reaction as click chemistry.[24] Cl-POSS is reactive to second substitution (S_N2) reactions,[31] which can be converted to Azide-POSS[32] for the Huisgen cycloaddition reaction as click chemistry.[33] Octasilicate is also known as a useful cage because it is possible to prepare from tetraalkoxysilane ($Si(OR)_4$).[34] As an example, octasilicate, (dimethylsiloxy)octasilicate (OS-$SiMe_2H$) is obtained by the reaction with chlorodimethylsilane ($ClSiMe_2H$).[35] OS-$SiMe_2H$ is functionalized by hydrosililation reactions.[35,36] Recently, Rh-catalyzed direct arylation of the Si–H bond at the corner of POSS was reported.[37] Several POSS derivatives are commercially available and they are applicable as a starting compound. By modulating introduction ratios and linking structures of 8 substituents in POSS, it is possible to obtain designed hybrid networks with diverse functions.

Figure 2

3. Chemical Sensors

3-1. Trapping Targets with Single POSS Molecule

Swager and co-workers proposed that π-conjugated polymers having bulky substituents were effective in developing chemical sensors.[38] The target should be recognized at the narrow space generated by bulky and rigid substituents. From this standpoint, the 3D dendritic structure of POSS is a potential scaffold for providing molecular recognition sites. Indeed, POSS-containing polymeric materials have been applied for gas sensors including amine, air, humidity by combining electronic devices or luminescent alterations.[39] Since the dendritic structure of POSS is favorable for presenting recognition sites among the POSS units, it is possible to efficiently capture the targets, such as organic substances[40] and metal ions.[41] For example, linear and reliable PL detection of D-glucose was achieved by using a phenylboronic acid-functionalized POSS.[40] Capturing metal ions, such as Cu^{2+},[41a,b] Fe^{3+},[41c] $Cr_2O_7^{2-}$,[41d] Hg^{2+},[41e] and Zn^{2+},[41f] among or into POSS-tethered luminophores possibly induced emission alteration of them. Moreover, by the combination with intrinsic characters of POSS, such as molecular rigidity, hydrophobicity and suppression of molecular motions, further properties are expected. In this section, unique optical properties induced by the accumulation of the chromophores onto POSS are illustrated.

Induction of excimer emission of polycyclic aromatic hydrocarbons such as pyrene and its application for a chemical sensor is described. Because the intensity ratio of dual emission from locally-excited (LE) and excimer states is sensitive to external stimuli and environmental changes, excimer is one of versatile luminescent processes for constructing chemical sensors.[42] Meanwhile, excimer can be observed only in the concentrated state because dimeric interaction of the dyes in the excited state is

necessary.[43] Moreover, molecular motions and diffusion should be suppressed for obtaining efficient excimer emission. By using POSS as a scaffold, these problems can be readily solved. By connecting to the POSS core, chromophores can be accumulated into the compact spaces and molecular tumbling is restricted.[26,28,44] Therefore it is expected that excimer emission can be observed even under the dilute condition. We synthesized pyrene-connected POSS (**PPOSS** (**1**)) in 65% isolated yield by using the Menshutkin reaction from **DMA-POSS** which had *N*,*N*-dimethylaminopropyl groups as the side chains (Figure 3a).[23] The obtained **PPOSS** was ionic compounds and showed good solubility in various solvents including water. In the photoluminescence (PL) measurements, it was found that the PL properties were drastically changed depending on the solvent polarity (Figure 3b). Emission intensity was maximized in chloroform, while only the monomer luminescence was exhibited in the aqueous solution. It was indicated that spatial distances between the ionic side chains can be regulated by electrostatic interaction (Figure 3c). In less polar solvents, the counter anion should be attracted to the vicinity of the quaternary ammonium group, which weakened the electrostatic repulsion to form the excimers. Conversely, in highly polar solvents, the counter anion should dissociate, followed by electrostatic repulsion between the cations. As a result, the formation of the intramolecular excimer should be suppressed. It should be emphasized that excimer emission was also observed with anthracene and naphthalene-modified POSS derivatives, meaning that molecular motions are highly restricted around the POSS core and POSS has the efficient property for recruiting excimer formation. Therefore, excimer emission can be observed even from smaller sizes of aromatic hydrocarbons. Furthermore, the excimer properties in aqueous solution of **PPOSS** were controllable by adding amphiphilic anions and polyanionic

compounds (Figure 3d). This system was remarkable responsiveness to SDS which is the conventional indicator of river pollutant. Among the side chains on POSS, the SDS molecules are invaded. Subsequently, intramolecular interaction between pyrene should be drastically enhanced by neutralization of static charges at the linkers. Finally, excimer formation should be allowed. From these results, around the POSS core, molecular motions can be efficiently suppressed even in the excited state. Interestingly, by external stimuli, this suppression effect is tunable.

Figure 3

Turn-off sensors were fabricated by using the interaction between luminophores and quenchers assisted by the POSS scaffold. Xu, Li and co-workers synthesized a dendritic organic–inorganic hybrid nanomaterial with 8 silole units covalently bonded to the POSS core (**2**) (Figure 4).[45] 2,3,4,5-Tetraphenylsilole is known to show the aggregation-induced emission (AIE) property. Due to intramolecular molecular rotations, weak emission is observed in the good solvent, while intense emission is obtained in the aggregation state by suppressing energy-consumable molecular motions.[46] The silole units were effectively introduced to the POSS core by using the hydrosilylation reaction in the presence of Karstedt's catalyst in 57% isolated yield. Indeed, **2** showed sky blue emission only in aggregate (THF/water = 1/9 v/v). Interestedly, emission in the aggregation state can be selectively quenched by addition of 2,4,6-trinitrophenol (picric acid, PA). By accumulating PA as a quencher and AIE-active silole derivatives on the POSS scaffold, excitation energy should be efficiently transported from silole to PA through electron transfer and fluorescence

resonance energy transfer (FRET) processes. As a result, selective quenching can be obtained. The system has the potential to prepare sensitive, selective, and stable sensors for the detection of explosives in aqueous media.[47] This study is the first example to offer the molecular recognition with POSS aggregates although further information should be needed to design sensors with same mechanism for different targets.

Figure 4

3-2. Trapping Targets with POSS Networks

In the previous section, it was described that unique optical properties, such as excimer emission and efficient energy transfer, can be induced from the chromophores by locating around the POSS core. Furthermore, these properties were dynamically controlled by changing environmental factors as well as external stimuli. In this section, the effect by POSS networks on the optical properties and stimuli-responsivity is explained. According to our previous works, it was indicated that encapsulation ability can be enhanced in the POSS network polymers.[7] On the basis of this fact, the POSS networks were synthesized by condensation reaction of Amino-POSS and bithiophene dicarboxylic acid as a linker (**3**, Figure 5a).[48] POSS networks having various cross-linking points with amide groups were obtained by modulating the feed ratio of the bithiophene dicarboxylic acid in the reaction. The obtained network polymers showed good water-solubility and strong blue emission derived from the bithiophene linker (Figure 5a). Interestingly, it was shown that the emission properties were changed by adding the silica particles (SPs) into the sample. It should be noted that the responsiveness was different depending on the size of SPs (Figure 5b). The red-shifted

emission of the POSS network was induced in the presence of the nanoparticles, while the blue-shifted emission was observed from the samples containing the microparticles. Plausible mechanism is illustrated in Figure 5c. In small-sized SPs, the hydrophobicity around the linker units could be enhanced, resulting in the observation of the red-shifted emission. On the other hand, in large-sized SPs, it is assumed that the linker units could be relatively isolated from the POSS core on the surface of SPs. Finally, the similar emission behavior to that of the free bithiophene carboxylic acid was observed from the POSS networks. In this study, it is demonstrated that optical properties of the chromophores were perturbed not by direct adsorption onto the particle surfaces but by microenvironmental changes inside POSS networks induced by the adsorption onto the particles. As a result, emission property changes, which are applicable not only for detecting water-pollution by particles but also for discriminating the size of the nanomaterials, can be obtained.

Figure 5

Next, by expanding the above results, we challenged detecting plastic particles and discriminating the kind of components as well.[49] The coumarin derivative was used as the environment-sensitive dye having the dual emission property consisting of blue emission from the intramolecular-charge-transfer (ICT) state and yellow one from the twisted-intramolecular-charge-transfer (TICT) state.[50] It should be mentioned that by introducing into POSS network, yellow emission, which can be observed under structurally-restricted condition, such as encapsulation into cyclodextrin, was exhibited. We prepared luminescent water-soluble networks containing the coumarin luminophore

(**CPN** (**4**)) by the condensation reaction of the Amino-POSS, coumarin D-1421 and succinic acid as a cross-linking point (Figure 6a). From the emission measurements, we found that the POSS networks showed bimodal emission bands in blue and yellow regions in water dispersion. In particular, enhancement of the emission band in the blue region was observed in the presence of polystyrene particles (PSPs) (Figure 6b). Similar behavior was observed by the addition of poly(lactic acid) particles (PLAPs) and poly(methyl methacrylate) particles (PMMAPs). In contrast, significant alterations were hardly observed by adding the SPs. Interestingly, plastic particles with the diameter less than 1 μm drastically affected optical properties of the networks. These data mean that the existence of plastic particles with sub-micron sizes in water was able to be detected with the POSS network by luminescent color changes from yellow to blue. Silica species, such as sand or rock particles, can be ignored in this system. From the mechanistic studies (Figure 6c), it was revealed that large enhancement of the blue emission from the ICT state in relatively small POSS networks (CPN-BE) was main reason of the color change when the networks were adsorbed onto the hydrophobic surfaces of the particles. Meanwhile, the yellow emission from the TICT state of relatively large POSS networks (CPN-YE) was scarcely affected by the circumstances because the large aggregates protected the emission moiety. Chemical sensors for nano-sized plastics, called as nanoplastics, were obtained based on the microenvironmental changes inside POSS networks induced by the adsorption of particle surfaces.

Figure 6

POSS-containing networks has been applied to molecular recognition of structural analogs of the significant compounds.[10–12] According to recent medical reports, a class of *trans*-fatty acids has been recognized as a harmful byproduct in food processing.[51] Thus, we aimed to establish the molecular recognition system via van der Waals interaction with POSS to achieve the *trans*-fatty acid discrimination with a fluorescent spectroscopy.[52] The water-soluble POSS network polymer connected with triphenylamine derivatives (**TPA-POSS** (**5**)) was prepared by the condensation reaction of Amino-POSS and 4,4′-(phenylazanediyl)dibenzoic acid (Figure 7a). The introduction ration of the TPA units was estimated to be 37% from ^{1}H NMR spectra. The sensing ability of the **TPA-POSS** to fatty acids was investigated. In the PL spectra, different time-dependent alterations of intensity as well as peak-top wavelengths were monitored from the solution coexisting **TPA-POSS** and oleic or elaidic acid which is mono-unsaturated fatty acid with 18 carbons as models of *cis*- or *trans*-fatty acid, respectively. After 24 h incubation, the PL intensity was reflected by the mixing ratios of *cis*- or *trans*-fatty acids, which was applied to quantitative detection of the ratios of isomerization (Figure 7b). From the mechanistic studies, it was implied that these changes could be derived from the difference in the degree of interaction between the POSS networks and each fatty acid. The *trans* isomer showed stronger affinity to the POSS networks because of relatively-larger aggregation formability than the *cis* isomer. Finally, *cis* and *trans* isomers can be discriminated according to emission intensity changes.

Figure 7

3-3. Controlling Molecular Mobility with POSS Networks

Molecular mobility of the encapsulated substituents in the POSS networks can be controlled by introduction of reactive chemical bonds at the linker. By introducing self-repair structure at the linker, reversible controls of molecular motions followed by optical properties can be realized. Since dissolved oxygen levels are critical indicators for detecting active tumor regions in vital bodies, stimuli-responsive materials depended on oxygen concentrations are directly used as a molecular probe.[53] There are a large number of hypoxia-selective luminescent probes based on oxygen quenching of phosphorescence.[54] To precisely estimate dissolved oxygen level, luminescent probes which can exhibit emission only under aerobic conditions are necessary. We showed a unique design for luminescent probes to detect high dissolved oxygen levels utilizing the POSS networks consisting of AIE-active dyes and disulfide linkers.[55] The AIE-active POSS network (**SSBKI-POSS** (**6**)) was synthesized by condensation reaction of Amino-POSS, AIE-active dye named boron ketoiminate (BKI),[56] 3,3′-dithiodipropionic acid as the redox-active linkers having a disulfide bond (Figure 8a). **SSBKI-POSS** showed greenish emission in water because the network structure restricted the molecular motion of the BKI moiety (Figures 8b and 8c). After addition of sodium ascorbate (SA) as the reagent for disulfide bond cleavage, the emission was quenched due to activated molecular motion of the BKI moiety by fragmentation of POSS networks. Under hypoxic condition, emission annihilation was continuously observed, meanwhile emission was gradually recovered under aerobic condition. By oxidation of the free thiol group, disulfide bonds were reproduced (Figure 8d). Subsequently, AIE should be obtained by structural restriction by the POSS unit in the

network. Thus, positive luminescent signals were obtained under not hyperoxic but aerobic condition.

Figure 8

3-4. Fluoride Sensors

Fluoride salts are commonly used as additives in drinking water or toothpaste owing to their beneficial effects on dental health. The U.S. Public Health Service affirmed the optimal level to be 1 mg of consumed fluoride anion (F^-) per day as an essential element of the body. On the other hand, excess ingestion of F^- can cause fluorosis, urolithiasis, or even cancer.[57] Therefore, development of the methods for the detection of F^- in water is required.[58] It was known that F^- has high affinity to silicon (Si) and there are many Si atoms in the POSS cages. When F^- is reacted with POSS cages, it is known that both encapsulation of F^- into POSS cages and degradation of POSS cages possibly occur.[59] Degradation of POSS cages is strongly induced by the condition of coexisting water because the resulting coexisting hydroxide (OH^-) trapped POSS fragments as siloxane derivatives (Si–OH). Therefore, the reactivity of POSS cage is available for selective detection of F^-.

In principle, the single F^- can induce environmental changes around the multiple substituents at the vertices after the chemical reaction with POSS. Therefore, the signal amplification followed by higher sensitivity can be expected from the POSS materials comparing to conventional sensors.

A turn-off F^- sensor of fluorescent POSS nanoparticle was designed by Bai and co-workers.[60] A perylene bisimide (PBI) having a polyethylene oxide (PEO) group was

used as a water dispersible luminescent dye and that was connected to POSS scaffolds by condensation reaction. The resulting mono-substituted POSS (**POSS-PBI-PEO** (**7**), Figure 9a) formed self-assembled nanoparticles (NPs). The cores of NPs are based on nanoscale cage-shaped POSS units, which can suppress the intermolecular π-aggregation and maintain the red excimer-like luminescence of PBI in the aggregation. However, addition of F^- to NPs caused partial or complete decomposition of POSS cages, and the resulting aggregation of PBI dyes showed quench of intense fluorescence of NPs. This new optical transduction mechanism was successfully accomplished and applied for the rapid detection of F^- in aqueous solution. In contrast, a turn-on sensor was also constructed by the use of POSS degradation triggered by F^-. Su, Li and co-workers prepared a hydrophilic luminescent network polymer composed of amino-functionalized POSS and perylene diimides (PDIs) by condensation reaction (**AE-PDI polymer** (**8**), Figure 9b).[61] The emission from PDI in the polymer turned off because of the photoinduced electron transfer (PET) between PDI and AE-POSS. After reaction with F^- in water, the fluorescent emission turned on obviously because the PET was blocked by the fragmentation of the network systems induced by degradation of the POSS cages. Selective detection of F^- was achieved and the system was inactive to the other anions such as Cl^-, Br^-, I^-, PO_4^{3-}, OH^-, SO_4^{2-}, SO_3^{2-}, NO^{3-}, and NO^{2-} (Figure 9b). Ren and co-workers developed POSS-end-capped PDI dyes for a turn-off or emission-color-change F^- sensor triggered by Si–O bonds cleavage.[62] They also fabricated the turn-on sensor by using the similar concept with an AIE-active dye composed of tetraphenylethylene connected by the POSS cage.[63]

Detection of F^- with emission color change was realized by controlling excimer emissions. Ervithayasuporn and co-workers proposed POSS cages as F^- sensors with

control of formation of pyrene–pyrene excimers.[64] Pyrene-modified POSS (**PySQ** (**9**), Figure 9a) was synthesized by the Heck reaction of vinyl-POSS and 1-bromopyrene. The modified POSS with average 4 equivalent of pyrene was obtained and showed the greenish excimer emission derived from pyrenes. The POSS selectively reacted to F^- and showed blue emission attributable to emission from the monomeric pyrene unit. The excimer emission control system was also applied to other hydrocarbons such as anthracene.[65] On the other hand, Tang, Xu and co-workers designed control system of the excimer emission with hydrogen-bonded organic framework (HOF) based on the pyrene-integrated POSS linked with amide groups.[66] The POSS derivatives **(POSS-(C_1-Py)$_8$** (**10**), Figure 9a) were prepared by condensation reactions between pyrenecarboxylic acid and amine-substituted POSS. The HOF nanoparticles showed apparent greenish emission of pyrene excimer. After reaction with F^-, the nanoparticles and the POSS cages were fragmented, and blue emissive pyrene-linked siloxanes was obtained. The fluorescence sensors based on HOF nanoparticles displayed insensitivity to the pH of solutions, sole selectivity to the F^-, and no response to the other anions such as Cl^-, Br^-, I^-, AcO^-, NO_3^-, ClO_4^-, and HPO_4^{2-}. In summary, the series of F^- sensors are described. The reaction of POSS with F^- followed by the cage degradation is responsible for optical changes. It should be noted that reaction with POSS can proceed even in the aggregation. As a consequence, signal amplification was accomplished.

Figure 9

3-5. Mechanical Sensors with Hybrid Polymers

Recent reports show that POSS derivatives with conjugated substituents can exhibit high affinity toward π-conjugated polymers. As a result, by using these POSS derivatives as a filler, thermally-stable polymer hybrids with π-conjugated polymers can be obtained.[6e,44f,44g] Furthermore, by modifying polyurethane ends with POSS, thermal stability and dispersibility of π-conjugated polymer into polyurethane (PU) films can be enhanced without significant losses of elasticity. PU is a well-known polymer material having high strength and flexibility.[67] In recent years, mechanochromic[68] and/or mechanochromic luminescent[69] materials has been fabricated with chromophore-loaded PUs. We designed elastic hybrid materials consist of POSS-capped polyurethane (**PUPOSS**) for reinforcing thermal stability by inhibiting pyrolysis at polymer ends.[70] A mono-functional POSS was used for the synthesis of **PUPOSS** (**11**), and POSS and PU were connected by condensation reaction (Figure 10a). According to the degradation temperature measurements, higher thermal stability was observed from **PUPOSS**. Furthermore, we discovered that PUPOSS has high compatibility with polyfluorene (PF). In the absence of the POSS unit, turbidity was observed, and elasticity was drastically spoiled. In contrast, the **PUPOSS** and PF blended film has high homogeneity according to microscopic observation and show similar elasticity to the pristine **PUPOSS**. The homogeneous films were readily obtained through simple mixing and dry process with **PUPOSS** and PF in organic solvents. The sample with 0.5 wt% PF (PUPOSS/PF) had good elasticity and exhibited dual emission from both LE and excimer states derived from PF.[71] Furthermore, the luminescent colors were varied by stretching the film samples attributable to alteration of the intensity ratio between the LE and excimer emissions (Figure 10). Moreover, similarly to conventional hybrid materials, hybridization mediated by POSS played significant roles in enhancement of

thermal stability, absolute PL quantum yields, mechanical properties and sensitivity. In contrast, hydrophobicity of POSS can induce aggregation of doped π-conjugated system such as polythiophene which increase electron conductivity without loss of stability. We fabricated stretchable and electric conductive hybrids consisting of **PUPOSS** and doped poly(3-hexylthiophene) (P3HT).[72] Homogeneous hybrid films were obtained by the simple mixing and drop-casting processes from the organic solutions. It was indicated that the resulting hybrid materials showed high conductivity and stretchability even with a small content of doped P3HT. It was suggested that POSS moieties promoted aggregation of doped P3HT in the films, and ordered structures should be involved in the aggregates. Therefore, efficient carrier transfer could occur through the POSS-inducible ordered structures in the aggregates. Our strategy based on the POSS-based hybrids is valid not only for tuning physical properties of polymers without spoiling intrinsic features but also for incorporating additional new functions. In these studies, POSS plays important roles in not only the improvement of compatibility of π-conjugated polymer into polyurethane but also excimer emission by assisting polymer assembly.

Figure 10

3-6. Thermally-Durable Mechanchromism

The mechanochomic luminescent material with thermal resistance is developed by using the POSS scaffold. Some emissive crystals showed luminochromic property during the transition to amorphous triggered by physical stresses such as pressing, crashing and grinding.[73] These mechanochromic luminescent behaviors are especially

beneficial for constructing pressure sensors as well as for fabricating optical memory devices. Although various types of mechanochromic luminescent behaviors have been reported so far, in the practical usages, thermally-durable mechanochromic luminescent materials are strongly required, such for a pressure-sensing paint in the wind-tunnel test.[74] From the degree of luminochromic behaviors, it is possible to estimate air-pressure even in the local spaces where electronic devices are not applicable. However, as is often the case with conventional crystalline organic materials, due to fraction heat inevitably generated by the air flow, recrystallization proceeds during measurements and subsequently the luminochromic behaviors are spoiled. As a consequence, the significant luminescent color changes disappeared. To solve this problem, we sought to improve the amorphous state by employing POSS.

We synthesized the solid-state emissive boron complexes and connected to each vertex of POSS (**M-POSS** (**12**)) by a cross-coupling reaction (Figure 11a).[30] The crystalline sample of **M-POSS** exhibited the bathochromic-shifted emission in comparison to that from the single molecule. By adding mechanical stresses to the crystalline sample, regular structures disappeared, followed by luminochromism from orange to yellow (Figure 11b). This result indicated that boron complexes linked to the POSS should be isolated from electronic interaction each other in the amorphous state after the grinding treatment. Interestingly, the emission color can be maintained by heating until melting. Conventional mechanochromic luminescent dyes tended to show reversible alterations by heating due to activation of molecular movement, meanwhile the POSS-tethered boron complex showed thermally-durable luminescent chromism. That is, the amorphous state can be stabilized and phase transition should be highly restricted by employing the POSS-based hybrid formation (Figure 11c).

Figure 11

4. Summary and Outlook

We mainly reviewed the recent studies of stimuli-responsive materials in which molecular assembly plays a key role in their properties. POSS is regarded as a scaffold for accumulating functional groups connected to the vertices. Moreover, by aggregation and dispersion, intrinsic unique properties of POSS, such as suppression of molecular motions, can be tuned. Based on these strategies, unique optical sensing has been accomplished. It is known that hybridization is one of typical strategies for obtaining robust materials, and environmental sensitivity is lowered in most cases of hybrid materials prepared with sol–gel reactions. Meanwhile, by employing POSS, hybrid materials can be obtained according to the design even with the substances which were not used in hybridization. As a result, unique behaviors have been discovered, as we partially introduced here.

POSS scaffolds can create the specific space which is not in other ones, and the space is valuable for designing stimuli-responsive materials. For example, POSS compounds form the stable aggregates in proper solvents and those enhance entrapping ability and sensitivity to the targets because of the dendritic structure and accumulated luminophores in comparison to non-POSS ones. However, control of aggregation and increase in sensitivity are still challenging tasks because the understanding how the steric effect of POSS cage and the connected luminophores work in solvents or film states is incomplete. Capturing the behavior should advance the sensing ability of POSS-based luminescent materials. Thus, we believe that a “designable hybrid” based

on a POSS element-block has tremendous potential to show further functions as well as multiple properties which can induce breakthrough in material science.

Acknowledgement

This work was partially supported by Scientific Research (A) (JSPS KAKENHI Grant Number, 21H02001), and a Grant-in-Aid for Scientific Research on Innovative Areas “New Polymeric Materials Based on Element-Blocks (No.2401)” (JSPS KAKENHI Grant Number P24102013).

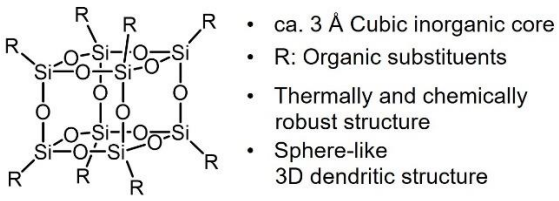

Figure 1. The characteristics of POSS scaffolds.

Table 1. The list of POSS compounds showing stimuli-responsive optical properties introduced in this review.

Compound	Luminophore	State	Sensor type	Emission type	Targets	Emission color	Ref.
1	Pyrene	Single molecule	Chemical	Dual	Sodium dodecyl sulfate (anionic surfactant)	Violet → Sky blue	[23]
2	Silole	Aggregate	Chemical	Turn-off	Picric acid (explosives, quencher)	Sky blue	[45]
3	Bithiophene	Network	Chemical	Color shift	Silica particle	Sky blue	[48]
4	Coumarin D-1421	Network	Chemical	Dual	Hydrophobic particle (nano plastic)	Yellow → Blue	[49]
5	Triphenyl amine	Network	Chemical	Color shift	Elaidic acid (*trans*-fatty acid)	Sky blue	[52]
6	Boron ketoiminate	Network	Chemical	Turn-off, Turn-on	Sodium ascorbate (reductant), Ammonium peroxodisulfate (oxidant)	Green	[55]
7	Perylene bisimide	Nanoparticle	Chemical	Turn-off	Fluoride anion	Red	[60]
8	Perylene bisimide	Polymer	Chemical	Turn-on	Fluoride anion	Yellow	[61]
9	Pyrene	Single molecule	Chemical	Dual	Fluoride anion	Sky blue → Violet	[64]
10	Pyrene	Hydrogen-bonded organic framework (HOF)	Chemical	Dual	Fluoride anion	Green → Blue	[66]
11	Polyfluorene	Hybrid film	Mechanical	Dual	Stretch	Yellow Green → Light Green	[70]
12	Boron ketoiminate	Crystal	Mechanical	Color shift	Grinding	Orange → Yellow	[30]

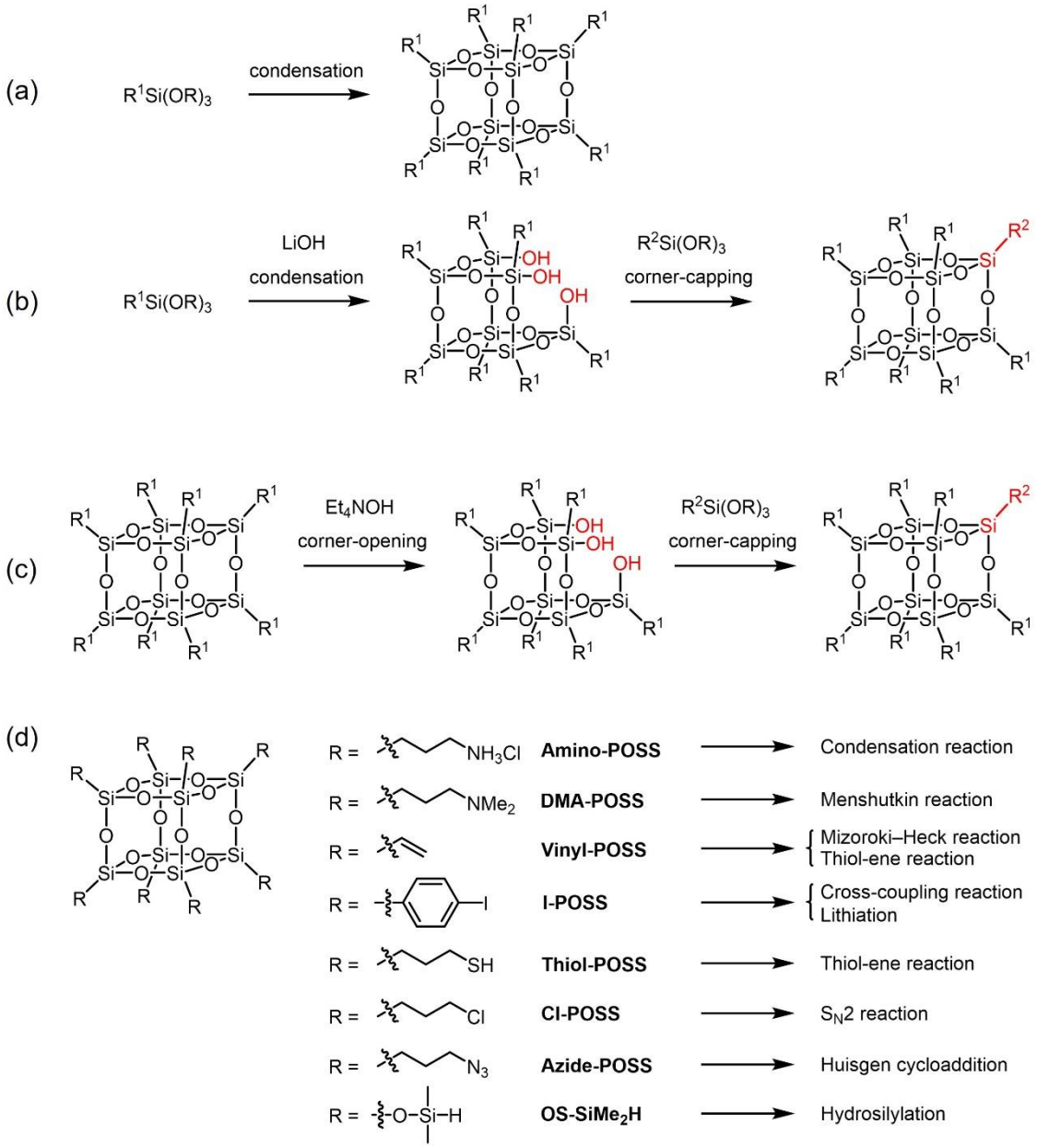

Figure 2. Synthetic schemes of POSS derivatives. (a) Condensation reaction for R_8T_8 structure. (b) Mono-substituted POSS by condensation reaction. (c) Mono-substituted POSS by corner-opening reaction. (d) Representative reactions for creating functional POSS derivatives.

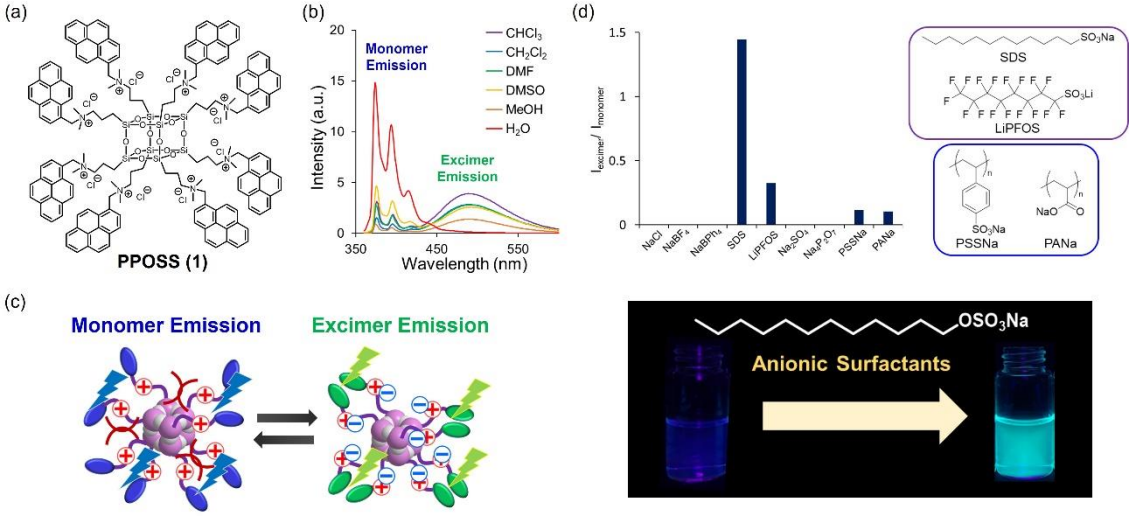

Figure 3. (a) Chemical structure of **PPOSS** (**1**). (b) PL spectra of **PPOSS** in various solvent (1.0×10^{-6} M). (c) Schematic illustration of emission switching of luminophore-integrated POSS. (d) Intensity of excimer to monomer emission of **PPOSS** aqueous solution (1.0×10^{-6} M) with various salts (1.0×10^{-4} M) excited at 349 nm and a photograph of the SDS detection by using **PPOSS**. Reprinted with permission from ref 23. Copyright (2018) The Royal Society of Chemistry.

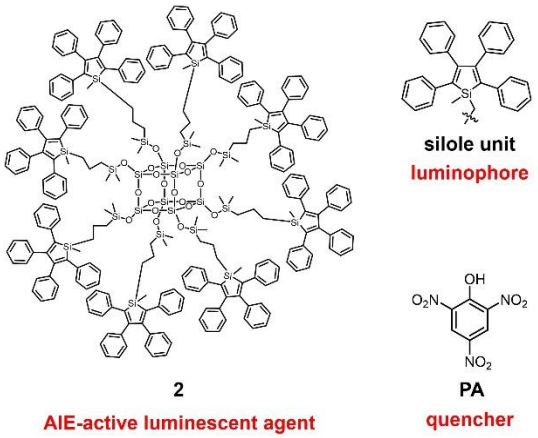

Figure 4. Chemical structure of the luminophore-integrated POSS derivative **2**, silole unit as a luminophore and quencher 2,4,6-trinitrophenol (PA).

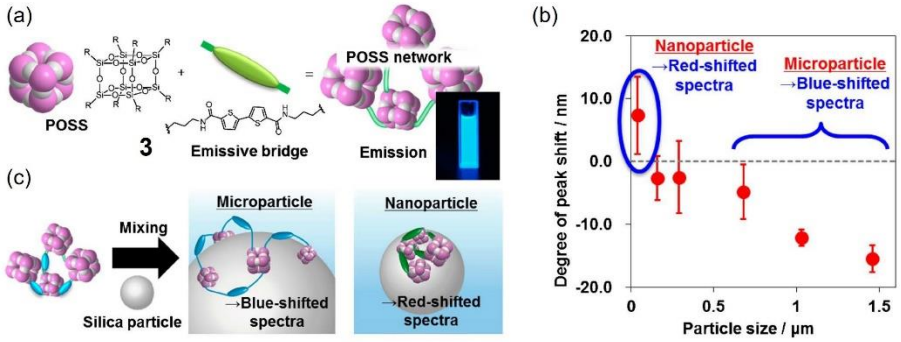

Figure 5. (a) Chemical structure of emissive POSS networks (**3**) for the size discrimination of silica particles. (b) Plausible mechanism for the detection. (c) Changes in the optical properties of POSS networks in the presence of various sizes of silica particles. Reprinted with permission from ref 48. Copyright (2015) The Royal Society of Chemistry.

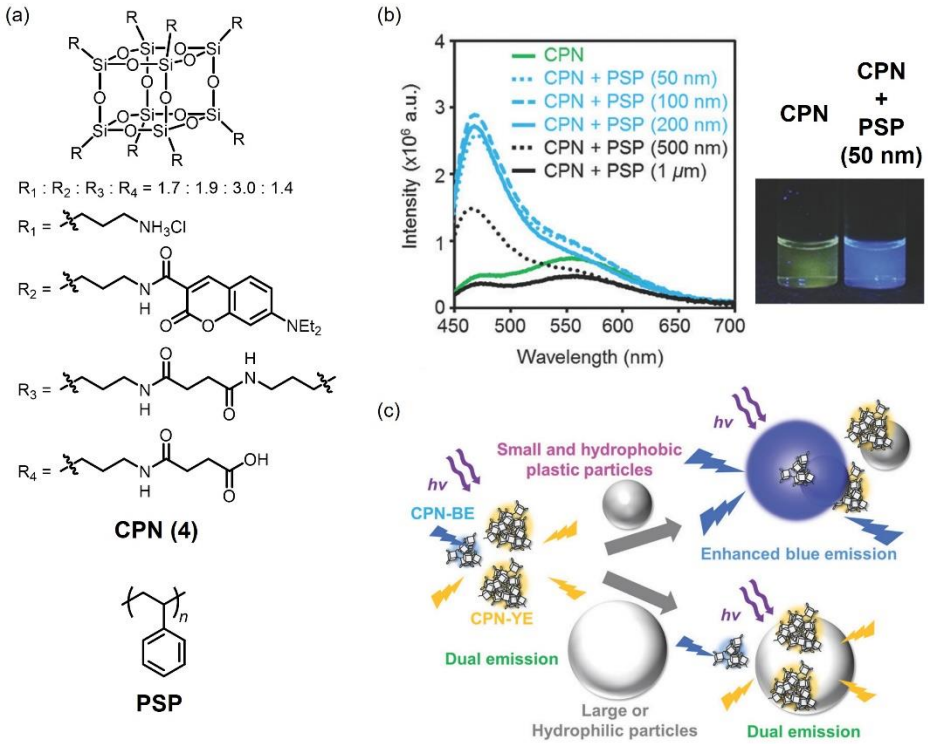

Figure 6. (a) Chemical structures of **CPN** (**4**) and polystyrene particle (PSP). (b) PL spectra of **CPN** (5 mM) in the presence of PSPs (c) A schematic model of the emission properties of **CPN** in the presence of particles. Reprinted with permission from ref 49. Copyright (2019) The Royal Society of Chemistry.

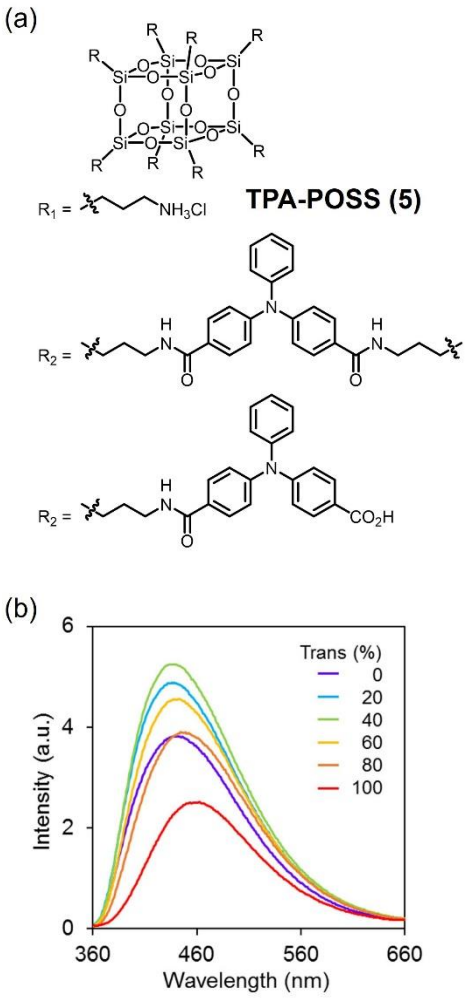

Figure 7. (a) Chemical structures of **TPA-POSS** (**5**). (b) PL spectra of **TPA-POSS** in the mixture samples containing both *cis*- and *trans*-fatty acids with various ratios in DMSO/H_2O (1/9, v/v) after 24 h incubation at 5 °C. The percentages represent the existing ratios of trans-fatty acid. Reprinted with permission from ref 52. Copyright (2017) Elsevier.

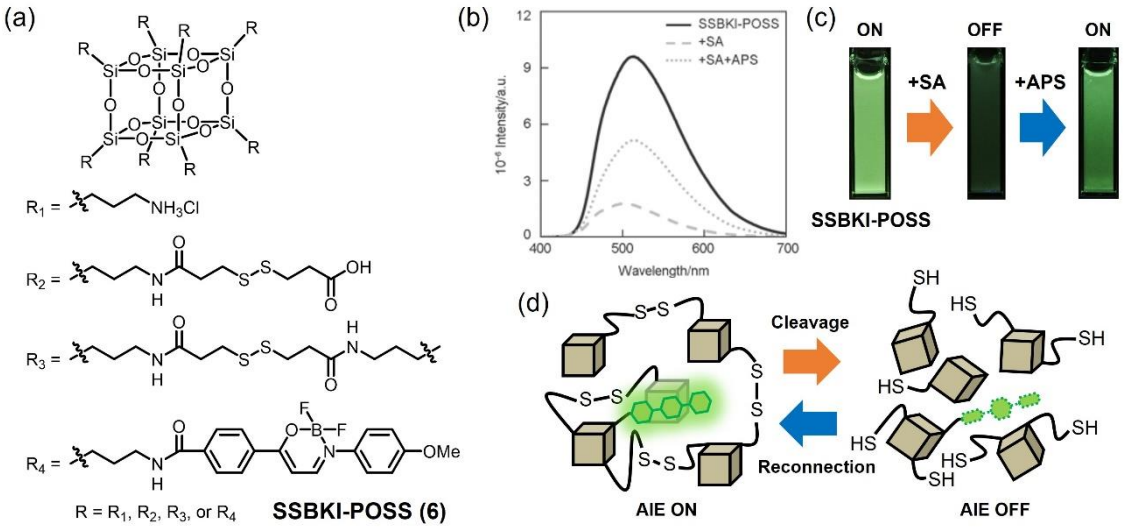

Figure 8. (a) Chemical structure of **SSBKI-POSS** (**6**). (b) PL spectra and (c) appearances under UV irradiation (365 nm) of **SSBKI-POSS** in water (0.25 mg/mL, BKI: 1.0×10^{-5} M) by tandemly adding sodium ascorbate (SA) (1.0×10^{-2} M) and followed by ammonium peroxodisulfate (APS) (1.0×10^{-2} M). (d) Schematic illustration of AIE on or off with stimuli-responsiveness. Reprinted with permission from ref 55. Copyright (2021) Springer.

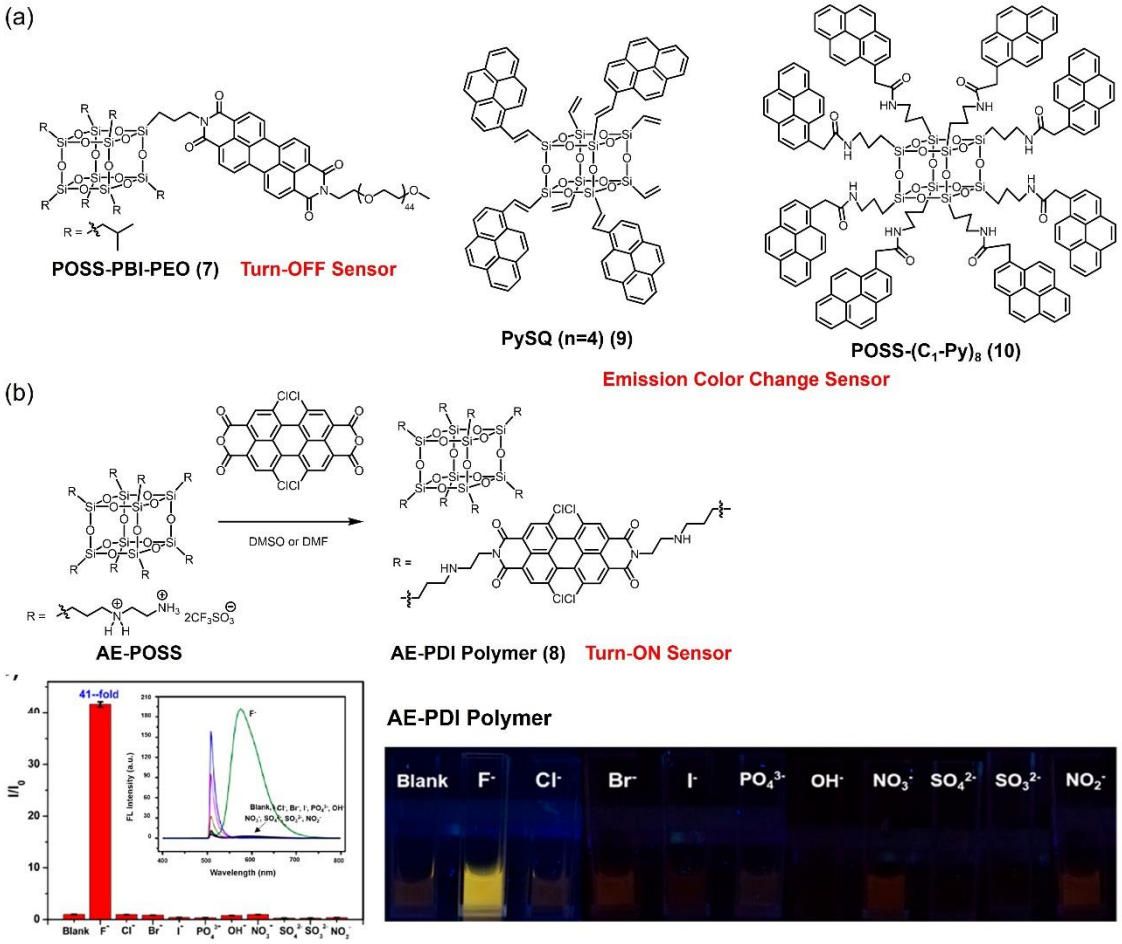

Figure 9. (a) Chemical structures of POSS derivatives (**7, 9, 10**) for F^- sensors. (b) Preparation scheme of **AE-PDI polymer** (**8**). Selectivity of **AE-PDI polymer** among different common anions. The PL spectra of the probe with addition of different anions and imaging of PL signals after addition of different anions to the probe solution under the irradiation of a UV lamp. Reprinted with permission from ref 61. Copyright (2020) American Chemical Society.

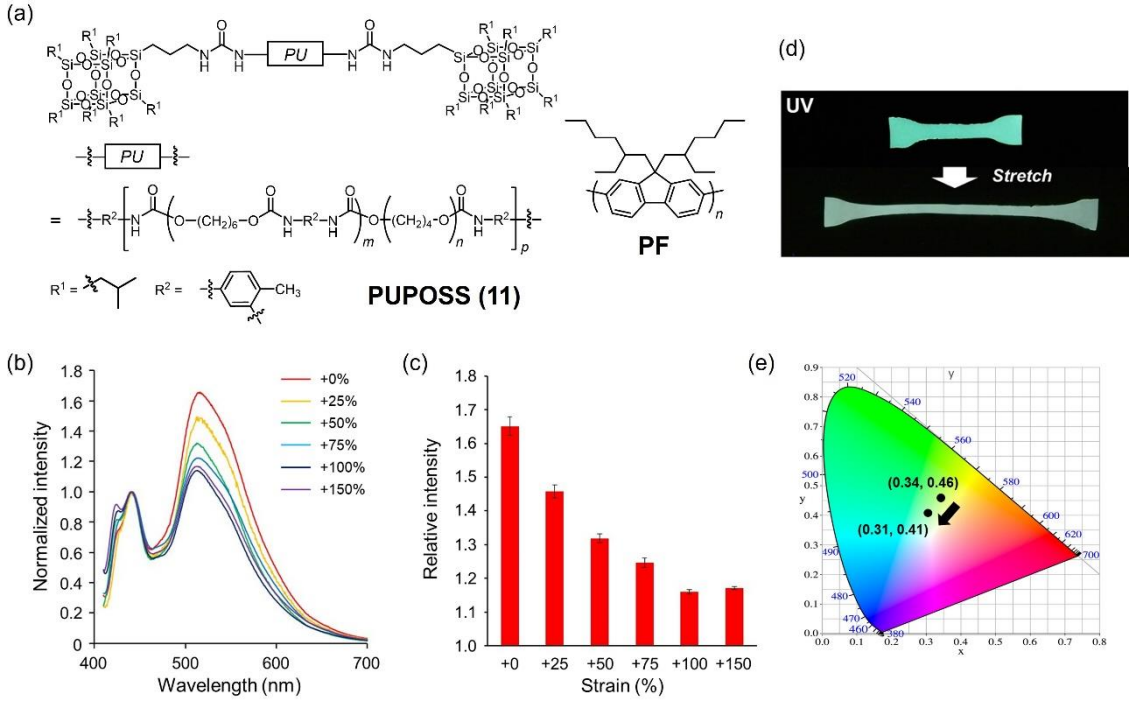

Figure 10. (a) Chemical structures of **PUPOSS** (**11**). (b) PL spectra of **PF/PUPOSS** at each strain. The spectra are normalized at the peak top wavelength of blue emission. (c) Relative intensity at the peak top wavelength of excimer emission at each strain. (d) A photo and (e) a CIE diagram of **PF/PUPOSS** stretched from 0% to 100% strain. Reprinted with permission from ref 70. Copyright (2019) The Royal Society of Chemistry.

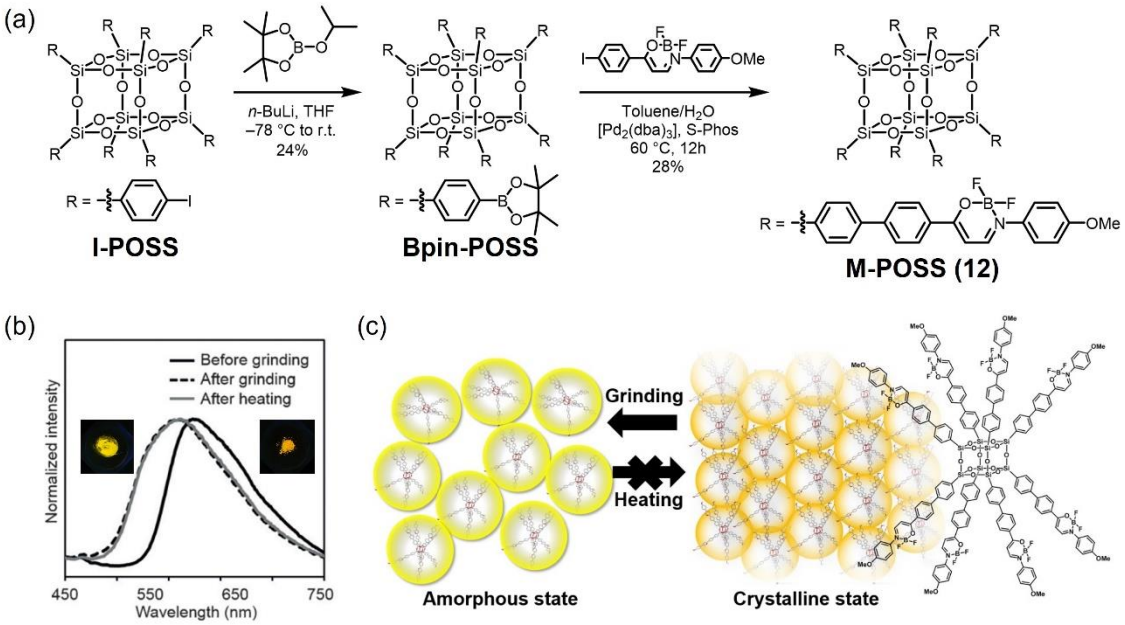

Figure 11. (a) Synthetic scheme of **M-POSS** (**12**). (b) PL spectra of M-POSS in solid states. The ground sample was heated at 200 °C for 10 min. THF vapor was fumed to the ground sample. Inserted photographs are **M-POSS** before and after grinding under visible and UV (365 nm) light irradiation. (c) Schematic illustration of heat-resistant mechanochromism of **M-POSS**. Reprinted with permission from ref 30. Copyright 2017 WILEY-VCH Verlag GmbH & Co. KGaA, Weinheim.

References

[1] a) X. Yan, F. Wang, B. Zheng, F. Huang, *Chem. Soc. Rev.* **2012**, *41*, 6042–6065; b) Zhang, J.; He, B.; Hu, Y.; Alam, P.; Zhang, H.; Lam, J. W. Y.; Tang, B. Z. *Adv. Mater.* **2021**, *33*, 2008071; c) X. Zhang, L. Chen, K. H. Lim, S. Gonuguntla, K. W. Lim, D. Pranantyo, W. P. Yong, W. J. T. Yam, Z. Low, W. J. Teo, H. P. Nien, Q. W. Loh, S. Soh, *Adv. Mater.* **2019**, *31*, 1804540; d) S. Ito, M. Gon, K. Tanaka, Y. Chujo, *Polym. Chem.* **2021**, *12*, 6372–6380; e) M. Gon, K. Tanaka, Y. Chujo, *Bull. Chem. Soc. Jpn* **2018**, *92*, 7–18; f) P. Iacomi, G. Maurin, *ACS Appl. Mater. Interfaces* **2021**, *13*, 50602–50642; g) G. A. Leith, C. R. Martin, A. Mathur, P. Kittikhunnatham, K. C. Park, N. B. Shustova, *Adv. Energy Mater.* **2022**, *12*, 2100441.

[2] a) Q. Yang, J. Li, X. Wang, H. Peng, H. Xiong, L. Chen, *Biosens. Bioelectron.* **2018**, *112*, 54–71; b) X. Chen, T. Pradhan, F. Wang, J. S. Kim, J. Yoon, *Chem. Rev.* **2012**, *112*, 1910–1956; c) M. Wang, G. Zhang, D. Zhang, D. Zhu, B. Z. Tang, *J. Mater. Chem.* **2010**, *20*, 1858–1867.

[3] a) M. Gon, S. Ito, K. Tanaka, Y. Chujo, *Bull. Chem. Soc. Jpn* **2021**, *94*, 2290–2301; b) K. Tanaka, Y. Chujo, *Polym. J.* **2020**, *52*, 555–566; c) M. Gon, K. Tanaka, Y. Chujo, *Polym. J.* **2018**, *50*, 109–126; d) Y. Chujo, K. Tanaka, *Bull. Chem. Soc. Jpn* **2015**, *88*, 633–643.

[4] a) D. B. Cordes, P. D. Lickiss, F. Rataboul, *Chem. Rev.* **2010**, *110*, 2081–2173; b) J. J. Schwab, J. D. Lichtenhan, *Appl. Organometal. Chem.* **1998**, *12*, 707–713; c) F. K. Wang, X. Lu, C. He, *J. Mater. Chem.* **2011**, *21*, 2775–2782. d) H. Shi, J. Yang, M. You, Z. Li, C. He, *ACS Mater. Lett.* **2020**, *2*, 296–316.

[5] K. Tanaka, Y. Chujo, *J. Mater. Chem.* **2012**, *22*, 1733–1746.

[6] a) E. Ayandele, B. Sarkar, P. Alexandridis, *Nanomaterials* **2012**, *2*, 445–475; b) I. Blanco, F. A. Bottino, *Polym. Compos.* **2013**, *34*, 225–232; c) K. Ueda, K. Tanaka, Y. Chujo, *Polym. J.* **2020**, *52*, 523–528; d) K. Tanaka, H. Kozuka, K. Ueda, J.-H. Jeon, Y. Chujo, *Mater. Lett.* **2017**, *203*, 62–67; e) K. Ueda, K. Tanaka, Y. Chujo, *Polym. J.* **2016**, *48*, 1133–1139; f) K. Tanaka, S. Adachi, Y. Chujo, *J. Polym. Sci. A Polym. Chem.* **2010**, *48*, 5712–5717; g) K. Ueda, K. Tanaka, Y. Chujo, *Polymers* **2018**, *10*, 1332; h) K. Ueda, K. Tanaka, Y. Chujo, *Bull. Chem. Soc. Jpn* **2017**, *90*, 205–209; i) J.-H. Jeon, K. Tanaka, Y. Chujo, *J. Polym. Sci. Part A: Polym. Chem.* **2013**, *51*, 3583–3589.

[7] K. Tanaka, Y. Chujo, *J. Mater. Chem.* **2012**, *22*, 1733–1746.

[8] a) K. Tanaka, K. Inafuku, K. Naka, Y. Chujo, *Org. Biomol. Chem.* **2008**, 6, 3899–3901; b) K. Tanaka, J.-H. Jeon, K. Inafuku, Y. Chujo, *Bioorg. Med. Chem.* **2012**, *20*, 915–919.

[9] K. Tanaka, N. Kitamura, K. Naka, M. Morita, T. Inubushi, M. Chujo, M. Nagao, Y. Chujo, *Polym. J.* **2009**, *41*, 287–292.

[10] K. Tanaka, M. Murakami, J.-H. Jeon, Y. Chujo, *Org. Biomol. Chem.* **2012**, *10*, 90–95.

[11] J.-H. Jeon, T. Kakuta, K. Tanaka, Y. Chujo, *Bioorg. Med. Chem. Lett.* **2015**, *25*, 2050–2055.

[12] J.-H. Jeon, K. Tanaka, Y. Chujo, *Org. Biomol. Chem.* **2014**, *12*, 6500–6506.

[13] T. Kakuta, H. Narikiyo, J.-H. Jeon, K. Tanaka, Y. Chujo, *Bioorg. Med. Chem.* **2017**, *25*, 1389–1393.

[14] a) P. G. Harrison, *J. Organomet. Chem.* **1997**, *542*, 141–183; b) T. Matsumoto, Y. Kaneko, *Bull. Chem. Soc. Jpn* **2019**, *92*, 1060–1067; c) M. F. Roll, J. W. Kampf,

Y. Kim, E. Yi, R. M. Laine, *J. Am. Chem. Soc.* **2010**, *132*, 10171–10183; d) S.-S. Choi, A. S. Lee, S. S. Hwang, K.-Y. Baek, *Macromolecules* **2015**, *48*, 6063–6070; e) V. Ervithayasuporn, S. Chimjarn, *Inorg. Chem.* **2013**, *52*, 13108–13112.

[15] K. Tanaka, K. Inafuku, S. Adachi, Y. Chujo, *Macromolecules* **2009**, *42*, 3489–3492.

[16] N. Prigyai, S. Chanmungkalakul, V. Ervithayasuporn, N. Yodsin, S. Jungsuttiwong, N. Takeda, M. Unno, J. Boonmak, S. Kiatkamjornwong, *Inorg. Chem.* **2019**, *58*, 15110–15117.

[17] S. Morimoto, H. Imoto, K. Kanaori, K. Naka, *Bull. Chem. Soc. Jpn* **2018**, *91*, 1390–1396.

[18] F. J. Feher, R. Terroba, J. W. Ziller, *Chem. Commun.* **1999**, 2309–2310.

[19] T. Maegawa, Y. Irie, H. Fueno, K. Tanaka, K. Naka, *Chem. Lett.* **2014**, *43*, 1532–1534.

[20] a) H. Zou, Q.-W. Li, Q.-L. Wu, W.-Q. Liang, X.-H. Hou, L. Zhou, N. Liu, Z.-Q. Wu, *Polym. Chem.* **2021**, *12*, 3917–3924; b) R. Kajiya, H. Wada, K. Kuroda, A. Shimojima, *Chem. Lett.* **2020**, *49*, 327–329.

[21] H. Imoto, S. Wada, K. Naka, *Chem. Lett.* **2016**, *45*, 1256–1258.

[22] N. Z. Menshutkin, *Phys. Chem.* **1890**, *5*, 589–600.

[23] H. Narikiyo, M. Gon, K. Tanaka, Y. Chujo, *Mater. Chem. Front.* **2018**, *2*, 1449–1455.

[24] a) T. Posner, *Ber. Dtsch. Chem. Ges.* **1905**, *38*, 646–657; b) C. E. Hoyle, C. N. Bowman, *Angew. Chem. Int. Ed.* **2010**, *49*, 1540–1573.

[25] a) T. Mizoroki, K. Mori, A. Ozaki, *Bull. Chem. Soc. Jpn* **1971**, *44*, 581–581; b) R. F. Heck, J. P. Nolley, *J. Org. Chem.* **1972**, *37*, 2320–2322; c) I. P. Beletskaya, A. V. Cheprakov, *Chem. Rev.* **2000**, *100*, 3009–3066.

[26] M. Y. Lo, C. Zhen, M. Lauters, G. E. Jabbour, A. Sellinger, *J. Am. Chem. Soc.* **2007**, *129*, 5808–5809.

[27] M. F. Roll, M. Z. Asuncion, J. Kampf, R. M. Laine, *ACS Nano* **2008**, *2*, 320–326.

[28] M. Gon, K. Sato, K. Tanaka, Y. Chujo, *RSC Adv.* **2016**, *6*, 78652–78660.

[29] K. C. Nicolaou, P. G. Bulger, D. Sarlah, *Angew. Chem. Int. Ed.* **2005**, *44*, 4442–4489.

[30] K. Suenaga, K. Tanaka, Y. Chujo, *Chem. Eur. J.* **2017**, *23*, 1409–1414.

[31] B. Marciniec, M. Dutkiewicz, H. Maciejewski, M. Kubicki, *Organometallics* **2008**, *27*, 793–794.

[32] W. Yuan, X. Liu, H. Zou, J. Li, H. Yuan, J. Ren, *Macromol. Chem. Phys.* **2013**, *214*, 1580–1589.

[33] a) R. Huisgen, *Proc. Chem. Soc.* **1961**, 357–396; b) H. C. Kolb, M. G. Finn, K. B. Sharpless, *Angew. Chem. Int. Ed.* **2001**, *40*, 2004–2021; c) J. R. Johansson, T. Beke-Somfai, A. Said Stålsmeden, N. Kann, *Chem. Rev.* **2016**, *116*, 14726–14768.

[34] I. Hasegawa, K. Kuroda, C. Kato, *Bull. Chem. Soc. Jpn* **1986**, *59*, 2279–2283.

[35] M. Dutkiewicz, H. Maciejewski, B. Marciniec, J. Karasiewicz, *Organometallics* **2011**, *30*, 2149–2153.

[36] J. Y. Corey, J. Braddock-Wilking, *Chem. Rev.* **1999**, *99*, 175–292.

[37] H. Imoto, S. Wada, K. Naka, *Dalton Trans.* **2017**, *46*, 6168–6171.

[38] a) J.-S. Yang, T. M. Swager, *J. Am. Chem. Soc.* **1998**, *120*, 11864–11873; b) D. T. McQuade, A. E. Pullen, T. M. Swager, *Chem. Rev.* **2000**, *100*, 2537–2574.

[39] a) A. Castaldo, L. Quercia, G. Di Francia, A. Cassinese, P. D'Angelo, *J. Appl. Phys.* **2008**, *103*, 054511; b) E. Massera, A. Castaldo, L. Quercia, G. Di Francia, *Sens. Actuators B Chem.* **2008**, *129*, 487–490; c) L. Lei, H. Ma, J. Lv, T. Wang, Y. Yang, P. Yin, Z. Lei, Y. Qin, Y. Ma, W. Yao, *React. Funct. Polym.* **2018**, *125*, 84–92; d) Y.-J. Lee, J.-G. Kim, J.-H. Kim, J. Yun, W. J. Jang, *J. Nanosci. Nanotechnol.* **2018**, *18*, 6565–6569; e) Y. Zuo, X. Wang, Y. Yang, D. Huang, F. Yang, H. Shen, D. Wu, *Polym. Chem.* **2016**, *7*, 6432–6436.

[40] Y. J. Kim, K. O. Kim, J. J. Lee, *Mater. Sci. Eng. C* **2019**, *95*, 286–291.

[41] a) H. Zhou, Q. Ye, X. Wu, J. Song, C. M. Cho, Y. Zong, B. Z. Tang, T. S. A. Hor, E. K. L. Yeow, J. Xu, *J. Mater. Chem. C* **2015**, *3*, 11874–11880; b) F. Zou, H. Ling, L. Zhou, F. F. Wang, Y. Li, *Dyes Pigm.* **2021**, *184*, 108840; c) W. Li, S. Feng, *Polymers* **2021**, *13*, 196; d) H. Dang, Y. Li, H. Zou, S. Liu, *Dyes Pigm.* **2020**, *172*, 107804; e) R. Kunthom, P. Piyanuch, N. Wanichacheva, V. Ervithayasuporn, *J. Photochem. Photobio. A: Chem.* **2018**, *356*, 248–255; f) C. U. Lenora, N. Hu, J. C. Furgal, *ACS Omega* **2020**, *5*, 33017–33027.

[42] a) S. Karuppannan, J.-C. Chambron, *Chem. Asian J.* **2011**, *6*, 964–984; b) S. Wang, Y. Yang, X. Shi, L. Liu, W. Chang, J. Li, *ACS Appl. Polym. Mater.* **2020**, *2*, 2246–2251.

[43] a) S. A. Jenekhe, J. A. Osaheni, *Science* **1994**, 265, 765–768; b) J. B. Birks, *Nature* **1967**, *214*, 1187–1190.

[44] a) K. L. Chan, P. Sonar, A. Sellinger, *J. Mater. Chem.* **2009**, *19*, 9103–9120; b) J. C. Furgal, J. H. Jung, T. Goodson, R. M. Laine, *J. Am. Chem. Soc.* **2013**, *135*,

12259–12269; c) C.-C. Cheng, Y.-L. Chu, C.-W. Chu, D.-J. Lee, *J. Mater. Chem. C* **2016**, *4*, 6461–6465; d) C. B. He, Y. Xiao, J. C. Huang, T. T. Lin, K. Y. Mya, X. H. Zhang, *J. Am. Chem. Soc*, **2004**, 126, 7792–7793; e) Y. Irie, T. Yamanaka, K. Naka, *RSC Adv.* **2016**, *6*, 8346–8353; f) M. Gon, K. Sato, K. Kato, K. Tanaka, Y. Chujo, *Mater. Chem. Front.* **2019**, *3*, 314–320; g) M. Gon, S. Saotome, K. Tanaka, Y. Chujo, *ACS Appl. Mater. Interfaces* **2021**, *13*, 12483–12490; h) H. Zhou, J. Li, M. H. Chua, H. Yan, Q. Ye, J. Song, T. T. Lin, B. Z. Tang, J. Xu, *Chem. Commun.* **2016**, *52*, 12478–12481.

[45] K. Xiang, Y. Li, C. Xu, S. Li, *J. Mater. Chem. C* **2016**, *4*, 5578–5583.

[46] a) J. Chen, C. C. W. Law, J. W. Y. Lam, Y. Dong, S. M. F. Lo, I. D. Williams, D. Zhu, B. Z. Tang, *Chem. Mater.* **2003**, *15*, 1535–1546; b) J. Mei, N. L. C. Leung, R. T. K. Kwok, J. W. Y. Lam, B. Z. Tang, *Chem. Rev.* **2015**, *115*, 11718–11940.

[47] a) K. Xiang, L. He, Y. Li, C. Xu, S. Li, *RSC Adv.* **2015**, *5*, 97224–97230; b) Y. Gao, W. Xu, D. Zhu, L. Chen, Y. Fu, Q. He, H. Cao, J. Cheng, *J. Mater. Chem. A* **2015**, *3*, 4820–4826; c) Q. Wang, M. Unno, H. Liu, *Materials* **2021**, *14*, 3815.

[48] T. Kakuta, K. Tanaka, Y. Chujo, *J. Mater. Chem. C* **2015**, *3*, 12539–12545.

[49] R. Nakamura, H. Narikiyo, M. Gon, K. Tanaka, Y. Chujo, *Mater. Chem. Front.* **2019**, *3*, 2690–2695.

[50] G. Ramakrishna, H. N. Ghosh, *J. Phys. Chem. A* **2002**, *106*, 2545–2553.

[51] a) C. Li, Y. Zhang, S. Li, G. Wang, C. Xu, Y. Deng, S. Wang, *J. Agric. Food Chem.* **2013**, *61*, 10392–10397; b) S. K. Gebauer, J.-M. Chardigny, M. U. Jakobsen, B. Lamarche, A. L. Lock, S. D. Proctor, D. J. Baer, *Adv. Nutr.* **2011**, *2*, 332–354.

[52] H. Narikiyo, T. Kakuta, H. Matsuyama, M. Gon, K. Tanaka, Y. Chujo, *Bioorg. Med. Chem.* **2017**, *25*, 3431–3436.

[53] a) T. Yoshihara, Y. Hirakawa, M. Hosaka, M. Nangaku, S. Tobita, *J. Photochem. Photobiol. C* **2017**, *30*, 71–95; b) D. B. Papkovsky, R. I. Dmitriev, *Cell. Mol. Life Sci.* **2018**, *75*, 2963–2980.

[54] a) E. Roussakis, Z. Li, A. J. Nichols, C. L. Evans, *Angew. Chem. Int. Ed.* **2015**, *54*, 8340–8362; b) Y. Jiho, R. Kurihara, K. Kawai, H. Yamada, Y. Uto, K. Tanabe, *Bioorg. Med. Chem. Lett.* **2019**, *29*, 1304–1307; c) D. Hara, Y. Umehara, A. Son, W. Asahi, S. Misu, R. Kurihara, T. Kondo, K. Tanabe, *ChemBioChem* **2018**, *19*, 956–962.

[55] K. Suenaga, K. Tanaka, Y. Chujo, *Chem. Res. Chin. Univ.* **2021**, *37*, 162–165.

[56] R. Yoshii, K. Suenaga, K. Tanaka, Y. Chujo, *Chem. Eur. J.* **2015**, *21*, 7231–7237.

[57] R. Hu, J. Feng, D. Hu, S. Wang, S. Li, Y. Li, G. Yang, *Angew. Chem. Int. Ed.* **2010**, *49*, 4915–4918.

[58] J. P. Hutchinson, C. J. Evenhuis, C. Johns, A. A. Kazarian, M. C. Breadmore, M. Macka, E. F. Hilder, R. M. Guijt, G. W. Dicinoski, P. R. Haddad, *Anal. Chem.* **2007**, *79*, 7005–7013.

[59] a) A. R. Bassindale, M. Pourny, P. G. Taylor, M. B. Hursthouse, M. E. Light, *Angew. Chem. Int. Ed.* **2003**, *42*, 3488–3490; b) S. E. Anderson, D. J. Bodzin, T. S. Haddad, J. A. Boatz, J. M. Mabry, C. Mitchell, M. T. Bowers, *Chem. Mater.* **2008**, *20*, 4299–4309.

[60] F. Du, Y. Bao, B. Liu, J. Tian, Q. Li, R. Bai, *Chem. Commun.* **2013**, *49*, 4631–4633.

[61] M. Sun, H. Liu, Y. Su, W. Yang, Y. Lv, *Anal. Chem.* **2020**, *92*, 5294–5301.

[62] a) T. Gao, W.-F. Zhou, Y. Zhao, L. Shen, W.-Y. Chang, R.-K. Musendo, E.-Q. Chen, Y.-L. Song, X.-K. Ren, *Chem. Commun.* **2019**, *55*, 3012–3014; b) H.-J. Ben, X.-K. Ren, B. Song, X. Li, Y. Feng, W. Jiang, E.-Q. Chen, Z. Wang, S. Jiang, *J. Mater. Chem. C* **2017**, *5*, 2566–2576.

[63] Y.-T. Zeng, S.-Y. Gao, K. Traskovskis, B. Gao, X.-K. Ren, *Dyes Pigm.* **2021**, *193*, 109491.

[64] S. Chanmungkalakul, V. Ervithayasuporn, S. Hanprasit, M. Masik, N. Prigyai, S. Kiatkamjornwong, *Chem. Commun.* **2017**, *53*, 12108–12111.

[65] a) S. Chanmungkalakul, V. Ervithayasuporn, P. Boonkitti, A. Phuekphong, N. Prigyai, S. Kladsomboon, S. Kiatkamjornwong, *Chem. Sci.* **2018**, *9*, 7753–7765; b) C. Wannasiri, S. Chanmungkalakul, T. Bunchuay, L. Chuenchom, K. Uraisin, V. Ervithayasuporn, S. Kiatkamjornwong, *ACS Appl. Polym. Mater.* **2020**, *2*, 1244–1255.

[66] H. Zhou, M. H. Chua, H. R. Tan, T. T. Lin, B. Z. Tang, J. Xu, *ACS Appl. Nano Mater.* **2019**, *2*, 470–478.

[67] H.-W. Engels, H.-G. Pirkl, R. Albers, R. W. Albach, J. Krause, A. Hoffmann, H. Casselmann, J. Dormish, *Angew. Chem. Int. Ed.* **2013**, 52, 9422–9441.

[68] H. Zhang, F. Gao, X. Cao, Y. Li, Y. Xu, W. Weng, R. Boulatov, *Angew. Chem. Int. Ed.* **2016**, *55*, 3040–3044.

[69] Y. Sagara, H. Traeger, J. Li, Y. Okado, S. Schrettl, N. Tamaoki, C. Weder, *J. Am. Chem. Soc.* **2021**, 143, 5519–5525.

[70] M. Gon, K. Kato, K. Tanaka, Y. Chujo, *Mater. Chem. Front.* **2019**, *3*, 1174–1180.

[71] J. C. Scott, G. Klalrner, R. D. Miller, D. C. Miller, *Macromolecules* **1999**, *32*, 361–369.

[72] K. Kato, M. Gon, K. Tanaka, Y. Chujo, *Polymers* **2019**, *11*, 1195.

[73] a) K. Suenaga, K. Tanaka, Y. Chujo, *Eur. J. Org. Chem.* **2017**, *2017*, 5191–5196; b) S. Ohtani, M. Gon, K. Tanaka, Y. Chujo, *Chem. Eur. J.* **2017**, *23*, 11827–11833; c) M. Yamaguchi, S. Ito, A. Hirose, K. Tanaka, Y. Chujo, *J. Mater. Chem. C* **2016**, *4*, 5314–5319; d) R. Yoshii, K. Suenaga, K. Tanaka, Y. Chujo, *Chem. Eur. J.* **2015**, *21*, 7231–7237; e) S. Saotome, K. Suenaga, K. Tanaka, Y. Chujo, *Mater. Chem. Front.* **2020**, *4*, 1781–1788.

[74] a) S. J. Yi, K. C. Kim, *J. Visualization* **2014**, *17*, 253–273; b) T. Cai, D. Peng, Y. Z. Liu, X. F. Zhao, *J. Visualization* **2016**, *19*, 383–392.

Graphical Abstract

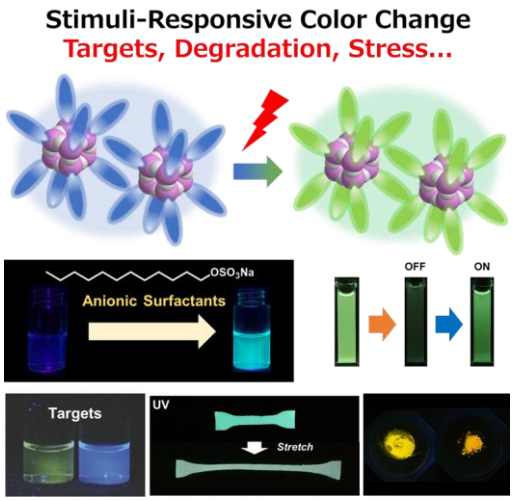

Recent progresses on the stimuli-responsive hybrid materials based on polyhedral oligomeric silsesquioxane (POSS) and their applications as chemical sensors are described. The unique functions originating from molecular assembly concerning POSS-containing soft materials are explained mainly from our studies.